Article:
Inaba, T., Archer, R.J., Gregory, D.A. et al. (2025) Lipid-hybrid multicompartment membrane systems for controlled, compartmentalized encapsulant release. Advanced Materials Interfaces, 12 (11). 2400959. ISSN: 2196-7350

https://doi.org/10.1002/admi.202400959

ADVANCED MATERIALS INTERFACES
Open Access
www.advmatinterfaces.de

Lipid-Hybrid Multicompartment Membrane Systems for Controlled, Compartmentalized Encapsulant Release

Tsuyoshi Inaba, Richard J Archer, David A Gregory, and Shin-ichiro M Nomura**

Multicellular structures are a common feature in biological organisms, conferring structural advantages including protection of internal content and spatiotemporal organization through defined spatial arrangements. Here a morphologically analogous lipid-hybrid multi-compartmental (LHMC) material produced within seconds on a milliliter scale by use of lipid and hydrophobic surfactant-rich oils referred to as "lipid-inks" is shown. This method encapsulates aqueous solutions at up to 94% of the total volume, into densely packed micro-compartments (20–200 µm) delineated by a continuous thin hydrophobic membrane. These LHMCs can be encased in hydrogel matrices for structural support and ease of handling. Controlled compartmentalized release of encapsulated content is demonstrated by triggered membrane solubilization from the introduction of hydrophilic surfactants to the external solution at or above their critical micellization concentration (CMC). Environmental ionic strength-dependent release rates are also demonstrated in the case of anionic sodium dodecyl sulfate (SDS). Notably, internal micro-compartments maintain content separation, enabling stable spatial patterning leading to controlled temporal release when directionally exposed to solubilizing agents. This micro-compartmentalized system, with its capacity for spatially and temporally regulated release and environmentally tunable rates, holds potential for advances in programmed delivery and responsive release of multiple bioactive agents in medical applications.

1. Introduction

Lipid bi-layer membranes form the essential structures of biological cells which encapsulate and protect the functional chemicals and processes within from dissipation and external environmental stressors.[1–3] These membranes are primarily formed by ambiphilic phospholipid biomolecules through simple hydrophobic forces, their thin layer morphologies with viscoelastic properties make them ideal as dynamic delineating structures.[4–6] Due to the natural tendency of phospholipids to self-assemble into enveloping structures in aqueous environments, extracted lipids can also form useful structures in vitro such as liposomes, which can be used for a wide variety of applications such as structural artificial cell models, delineated chemical reactions and biomimetic soft robots.[7–11] Liposomes, which can envelope hydrophilic chemicals, can also be used as drug delivery vectors to increase cellular uptake and bypass biological barriers due to their biocompatibility.[12–14] A key feature of complex life is the multicellular structure which serves a number of important functions, such as separation of function and optimization of microenvironments.[15,16] Importantly, compartmentalization also adds a spatial order to structures which is essential for temporal control and systematic processes, such as brain and nerve functions.[17,18] The lipid-based membrane compartmentalization could also be used in bio-inspired synthetic materials to control the spatial ordering and conferring temporal control.[19–23] In the field of drug delivery the ability to control release triggers and release rates can improve efficacy and utility. Spatial patterning of delivery devices can prove simple and effective mechanism for control over drug delivery.[24] For example, polypills can spatially arrange several medications within one capsule, with release orders and rates dependent on the initial spatial patterning.[25–29] Hydrogels and patch-like transmembrane delivery systems can demonstrate a matrix-assisted release with a passive or active release such as thermo-responsive, electro-responsive, or piezo-responsive release triggers,[30–33] however, due to the reliance on a continuous diffusible matrix, spatial separation and temporal control of release remains challenging.

T. Inaba, R. J. Archer, S.-i. M. Nomura
Department of Robotics, Graduate School of Engineering
Tohoku University
Sendai 980–8579, Japan
E-mail: archer.richard.james.c8@tohoku.ac.jp;
shinichiro.nomura.b5@tohoku.ac.jp

D. A. Gregory
School of Chemical, Materials and Biological Engineering
University of Sheffield
Sheffield S1 3JD, UK

D. A. Gregory
Insigneo Institute for in Silico Medicine, Pam Liversidge Building,
Sir Robert Hadfield Building
University of Sheffield
Sheffield S1 3JD, UK

The ORCID identification number(s) for the author(s) of this article can be found under https://doi.org/10.1002/admi.202400959

DOI: 10.1002/admi.202400959

Recently, we have developed a bio-inspired thin-layer multicompartmental structure from a combination of hydrophobic surfactants and naturally derived phospholipids, which display.[19,34] The lipid-hybrid material enables microcompartmentalization of aqueous contents, however, we note here that the LHMC system is chemically and functionally distinct from biological cells and pure lipid-prepared vesicles.

The 2D multicompartment structure was built to centimeter scales on a water-air interface, comprised of microscale lipid-hybrid compartments self-assembled by hydrophobic forces. The compartments could be physically arranged by simple pipetting and the ordering persisted over time without mixing of internal contents, giving user-directed spatial designs. Since the original report the fabrication procedure has been updated with dramatic improvements in efficiency, scale of production, and ease of synthesis. Here we show a proof of concept for lipid-hybrid membrane-based micro-compartmentalization based on the previously reported multicompartmental material, with updated methodology. In this report, we explore the application of these lipid-hybrid membranes as an efficient encapsulating material with facile user-directed spatial patterning which can lead to temporal control of release after membrane destruction. These synthetic lipid-hybrid membranes can be structurally reinforced by an agarose extracellular matrix which allows for easy handling. Using membrane solubilization techniques, the release of encapsulated content is found to occur on a sequential compartment by compartment basis in order of exposure to the environment. Membrane solubilization by the common surfactant sodium dodecyl sulfate (SDS), is found to be dependent on both surfactant concentrations and concentration of ionic species in the environment, giving a possible route to environmental and physiologically relevant triggers of release.

2. Results and Discussion

2.1. LHMC Formation by Lipid-Inks

LHMC formation was achieved by vortexing the desired aqueous solutions with lipid-inks as described in method section. For demonstrations of scale and determination of morphology, milliliter volumes of LHMC were prepared using hydrophilic calcein green and hydrophobic Nile red fluorescent dyes to image the encapsulated aqueous phase and the lipid-hybrid hydrophobic phase respectively. After vortexing the lipid-ink (12% unless otherwise stated) and the aqueous calcein green (88% unless otherwise stated) together for 10 s, the solution changed from two transparent immiscible liquids to a single homogenized solution with a cloudy appearance. We note here that while 12% lipid-ink was used in the following experiments, LHMC formation could be achieved with as little as 5% lipid-ink could be achieved by gradual addition of the aqueous phase. 1 mL of calcein green encapsulated LHMC was pipetted underwater directly onto a submerged glass slide in a petri dish. By manual manipulation, the LHMC could be patterned or covered over the glass slide in a thin layer-like painting (**Figure 1a**). During deposition, no breakage of the structure was visibly observed and the structure appeared stable over several weeks at room temperature. Morphology of the LHMC was determined by confocal microscopy, revealing the material was comprised of aqueous micro-compartments

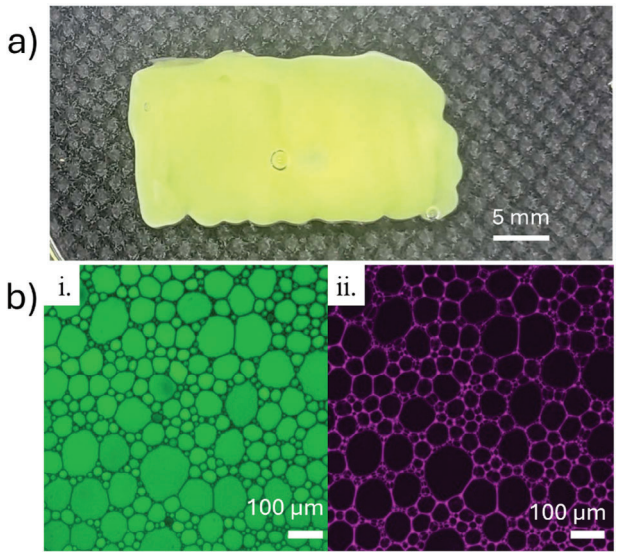

Figure 1. (a) LHMC, 88% aqueous calcein green fluorescent dye (100 uM), 12% hexadecane with POPC (6.5 mM) and SPAN 80 (2%), pipetted onto a glass slide (32 × 22 mm) underwater. (b) Confocal microscopy of LHMC, left: hydrophilic calcein green dye (Ex 494 nm) and right: hydrophobic Nile red dye (Ex 559 nm) with average compartment diameters and volumes of 82 μm (± 66 μm) and 1.4×10^{-4} μL (± 3.3×10^{-4} μL) respectively.

from 20 to 200 μm in diameter surrounded by hydrophobic thin layer (Figure 1b, i and ii), No fusion or breakage of the microcompartments was observed during microscopic analysis under standard conditions. The structures reported here have identical morphology to our previous reports on formation from lipid stabilized droplet coalescence from volatile oils.[19,34] The lipid-ink method could easily prepare over 8 mL of LHMC per 1 mL of lipid-based oil used against the 70 μL of LHMC produced per 1 mL of oil for the droplet coalescence. Furthermore, without the necessity for volatile oil evaporation which the coalescence method requires, the lipid-ink method can use non-volatile oil such as the hexadecane used in the present study and does not require a water-air interface for assembly. The lipid-ink procedure therefore offers vastly enhanced efficiency of formation and more convenient application as it is already fully formed after vortexing and can be more easily manually manipulated.

2.2. Encapsulant Release

To investigate membrane solubilization and subsequent encapsulant release by surfactant, LHMC (200 μL) containing Allura Red (AR) dye (1 mg mL^{-1}) was encased in agarose (2%) as described in the methods section (LHMC-agarose) and submerged in aqueous solutions containing various concentrations of sodium dodecylsulfate (SDS, 0.0–10.0 mM). Release of the encapsulated AR dye was monitored at 12-hour intervals by UV-vis spectroscopy on samples of the external aqueous solution. **Figure 2a** shows AR concentration in the outer aqueous solution as a function of time against SDS concentration. With LHMC-agarose in only DI-H_2O (SDS 0.0 mM) no significant concentrations of AR were measured after 72 h. Even after a significantly

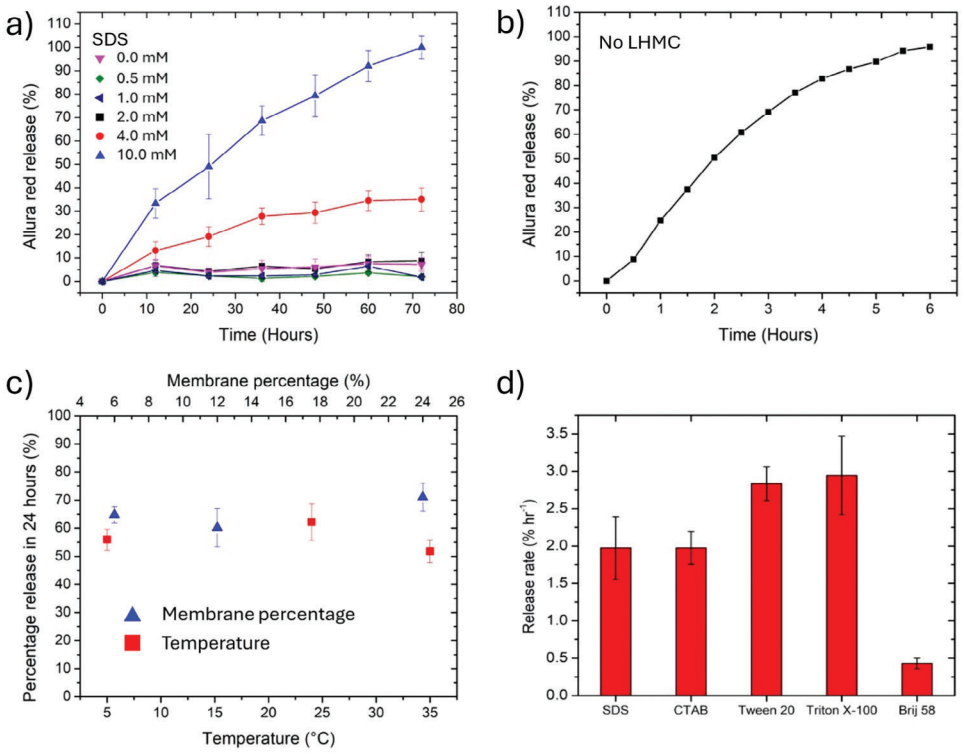

Figure 2. (a) Allura Red release from LHMC-agarose when the external solution is SDS in DI–H_2O. (b) Allura Red release from agarose with no LHMC and only DI-H_2O external solution. (c) Allura Red release from LHMC-agarose with an external solution of 10 mM SDS at different temperatures with 12% membrane lipid-ink and different percentages of membrane forming lipid-ink added at room temperature. d) Release rate of encapsulants from LHMCs using different surfactants at 10 mM.

longer time scale of 6 months, the LHMC retained their encapsulated dyes and AR could not be detected in the outer solution. When SDS was introduced in low concentration, up to 2 mM, no significant AR concentration was detected in the outer solution after 72 h and the LHMC structure within the agarose was visibly unchanged. At 4 mM SDS however, ≈13% of total encapsulated AR was detected in the outer solution from 12 h and this steadily increased up to 35% at 60 h after which the release of AR seemed to plateau, with no further change even beyond 72 h, this may indicate an increase in permeability of the membrane exposed to the external solution without destruction. At 10 mM SDS, ≈33% of AR is released within the first 12 h and steadily increases to ≈100% after 72 h. These experiments showed that LHMC-agarose is naturally stable in aqueous environments but that a surfactant (SDS) can destabilize the membrane when the concentration is near the CMC and solubilize the membrane at or above the CMC point as has been reported elsewhere.[35]

For comparison, Allura Red (1 mg mL^{-1}) without LHMC encapsulation was added to the agarose holders using the same procedure but without applying the lipid-inks (Figure 2b). The AR-agarose systems were placed in external solutions of DI-H_2O (**Figure** 3b). Measurements on the external solutions were taken every 30 m. In DI-H_2O only without any surfactant, AR was nearly all released into the environment within 6 h, these results demonstrate that agarose did not measurably retain AR. Significantly, the rate of release of AR from agarose without surfactant was significantly faster than even the highest release rates from LHMC-agarose devices, with an approximate 95% release at 6 h for AR in agarose versus 72 h at 10 mM SDS for LHMC-agarose. These results indicate that while agarose plays some role in rate of release, it is not the rate-limiting factor.

To investigate the influence of temperature on membrane solubilization and release of encapsulants, LHMC-agarose submerged in SDS (10 mM) were kept at 5, 24, and 35 °C. The AR release after 24 h showed no significant difference between the temperature ranges. Within practical temperature ranges, the LHMC membrane solubilization is not susceptible to differences in temperatures (Figure 2c). The influence of membrane thickness was also assessed by changing the ratio between the lipid-oil phase and the aqueous, 6:94, 12:88, and 24:76 respectively. LHMC-agarose with different lipid phase ratios were again added to solutions of SDS (10 mM) at room temperature, and their release percentage after 24 h were compared. Lipid-oil phase ratios had little to no influence on the release rate (Figure 2c). The influence of the surfactant type was investigated by submerging LHMC-agarose containing dye (AR, 1 mg mL^{-1} unless otherwise stated) into different surfactants with a set concentration of 10 mM and the release rate was monitored over 24 h (48 h for Brij 58 due to slow release) (Figure 2d). Cationic Cetyltrimethylammonium bromide (CTAB) was monitored through releasing encapsulated methylene blue dye (MB, 0.4 mg mL^{-1}) due to interactions between AR and CTAB causing insoluble precipitates. The release rate between anionic SDS and cationic CTAB was almost identical at 1.98%

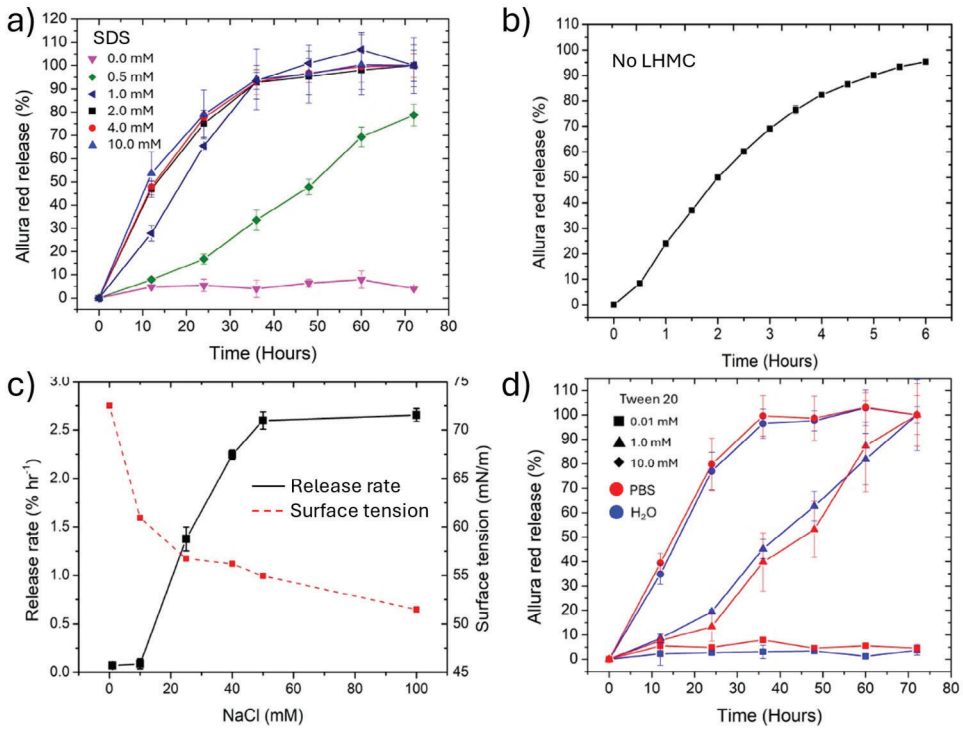

Figure 3. (a) Allura Red release from LHMC-agarose when an external solution is SDS in PBS. (b) Allura Red release from agarose with no LHMC and only PBS external solution. (c) Allura Red release from LHMC-agarose with an external solution of 2 mM SDS at different concentrations of NaCl, overlayed with surface tension. (d) Allura Red release from LHMC-agarose with an external solution of Tween 20 at 0.01 mM (square), 1.0 mM (triangle), or 10.0 mM (diamond) in either DI-H_2O (blue) or PBS (red).

per hour each, suggesting that the charge of the surfactant was not influential to the membrane solubilization. Tween 20, Triton X-100, and Brij 58 were selected as representatives for non-ionic surfactants. Tween 20 and Triton X-100 showed similar release rates at 2.83% per hour and 2.95% per hour respectively, ≈40% faster than the ionic SDS and CTAB surfactants. Brij 58 however, although also a non-ionic surfactant demonstrated a far slower release of ≈0.43% per hour. These results show that the choice of surfactants can influence the release rate.

2.3. Membrane Solubilization Mechanism

Membrane solubilization by SDS experiments was repeated with the introduction of a phosphate-buffered saline (PBS, 155.1 mM NaCl, 2.96 mM Na_2HPO_4, 1.06 mM KH_2PO_4) solution to investigate the effect of high ionic strength solutions and physiological conditions on membrane solubilization by SDS (Figure 3a). When submerged in a PBS solution but no addition of SDS (SDS 0 mM), the LHMC structure remains intact and no detectable AR is measured in the outer solution over 72 h or even after several weeks as observed by eye. We infer from this that ionic buffers themselves have no detrimental effect on the LHMC lipid-hybrid membranes. Interestingly, however, with the addition of SDS in the presence of PBS solution, the release of AR from the LHMC structure occurs with much lower concentrations of SDS. With as little as 0.5 mM SDS in PBS solution, a steady release of ≈10 – 15% of AR being released per 12 h for up to 72 h. 1 mM SDS in PBS solution showed a dramatic rate increase of ≈30% of AR releases for the first 36 h and a slower release thereafter. From 2 to 10 mM SDS in PBS solution the release pattern is almost indistinguishable, seemingly representing the fastest possible rate of LHMC membrane solubilization by SDS given the other experimental parameters (room temperature, surface area to volume ratio), with ≈45–50% of AR released in the first 12 h, 75– 80% of AR released by 24 h and a gradual release up to 100% AR release by 72 h. From these experiments, we show high ionic strength saline solutions have a significant effect on membrane solubilization and release of encapsulated contents in the presence of SDS anionic surfactant. This effect is suspected to be due to the high salt concentration causing electrostatic screening effects on the ionic molecules (SDS, POPC), reducing electrostatic repulsion and changing the CMC value of SDS.[36] The PBS buffer had no effect on the agarose casing or diffusion through agarose as shown by the rate of release of AR without LHMC encapsulation (Figure 3b), which showed no significant difference than release from DI-H_2O. The effect of solution ionic strength on dissolved charged molecules is well documented, including, increased electrostatic screening (lowering repulsive and attractive ionic associations), changing solubility, and lowering the CMC point for surfactants.[37,38] In the case of SDS and LHMC membranes, both the surfactant and the phospholipids are charged molecules, therefore the exact effect of the high ionic strength PBS solution on membrane solubilization by SDS is unknown as the lipid-hybrid membrane, the surfactant CMC and surfactant-membrane electrostatic interactions are likely all affected.

To clarify the relationship between ionic strength and SDS-based solubilization of the LHMC membranes, AR release rate experiments were conducted against a range of concentrations of the monovalent salt sodium chloride (Figure 3c). LHMC-agarose (200 µL, 2 wt.% agarose) with encapsulated AR (1 mg mL^{-1}) was exposed to solutions of 2 mM SDS at 10, 25, 40, 50, and 100 mM NaCl. The rate of release of AR was found by determining the gradient of AR release between 12 and 36 h, where the AR release is approximately linear. With 10 mM NaCl, no significant release of AR was observed over the course of the experiment. Increasing the NaCl concentration to 25 mM showed a dramatic increase in the release rate of AR to ≈1.4% per hour, at 40 and 50 mM this further increased to 2.3% and 2.6% per hour respectively, after which the release rate no longer increased with increasing NaCl concentration. The maximal release rate at 50 mM NaCl aligns with the reported CMC point of 2 mM SDS at 50 mM NaCl.[39] From our own experimental measurements of the surface tension by employing the Du Noüy method, the surface tension of 2 mM SDS rapidly decreases with the addition of 10 mM NaCl and begins to plateau at 25 mM NaCl, suggesting that this is at least may be the onset of micelle formation. The presence of micelles at 2 mM SDS and salt concentrations between up to 100 mM was further investigated by dynamic light scattering (DLS), from which a light scattering signal was detected from 40 mM NaCl at 1 nm, and progressively grew in size to ≈5 nm at 100 mM NaCl, which matched the DLS peak for 10 mM SDS in DI-H_2O (Figure S1, Supporting Information). From these results, the onset of micellization of SDS as measured by Du Noüy surface tension measurements appeared to match with the onset of membrane breakdown and release of encapsulants, and the growth of micelles into well-defined structures as determined by DLS matched with the plateau in release rate.

To investigate the effect of high ionic strength solutions on the LHMC lipid membrane itself, the SDS surfactant was changed for the non-ionic surfactant Tween 20 (CMC ≈ 0.06 mM), thereby reducing the ionic molecules to only the salt and the zwitterionic POPC phospholipids. LHMC-agarose (200 µL encapsulated in 2% agarose) containing AR (1 mg mL^{-1}) was exposed to solutions containing Tween 20 at 0.01, 1, and 10 mM (below, above, and far exceeding the CMC respectively) either in H_2O or a PBS solution (Figure 3d). Again, the AR value is taken as the total amount of AR derived from the concentration measured from UV-vis spectroscopy and known total volume. Figure 3d shows that for LHMC-agarose in 0.01 mM Tween 20, no significant of AR is recorded over 72 h. For 1 mM a steady release of ≈20% every 12 h is recorded and for 10 mM a rapid release of ≈40% per 12 h is measured for the first 24 h followed by a slower release rate to a full release sometime between 36 h to 72 h. Notably these trends are indistinguishable between samples in DI-H_2O or PBS solutions. From these results, we infer that the high ionic solutions have no detrimental effect on the membrane's stability and that solubilization is entirely dependent on the surfactant and specifically on the formation of surfactant micelles.

2.4. Physical Mechanism of Release

Unlike biological multicellular tissues which are interconnected discrete membranes, The LHMC system contains discrete internal sections with continuous phase outer membrane. As the surfactant molecules are not thought to pass through the membranes then compartment destruction and release would occur in order of exposure to the environment (**Figure** 4a). Fluorescence microscopy was used to observe and investigate the physical breaking mechanism of a multicellular system with a continuous membrane. Microscopy observations were conducted with fluorescent calcein and Nile red LHMC on glass slides under water. Submerged calcein-LHMC under water when exposed to Tween 20 (10 mM) confirmed the release of encapsulated content occurs by individual compartment breakage with the edges of the structures, with the highest exposure to the external solution was observed to break first, releasing the encapsulated dye (Figure 4b). While individual compartments were observed to break within fractions of a second, major deterioration of the overall lipid structure was observed to occur over much longer time scales from s to m for major structural changes (Figure 4c). We hypothesize that surfactants can insert into the exposed membrane section until they reach an environmentally influenced critical concentration to form a micelle which can solubilize the membrane.

2.5. Spatial to Temporal Release

Exploiting the spatially restricted release of LHMC encapsulants through directional membrane solubilization can result in temporal release patterns. Two LHMC solutions containing either AR or methylene blue (MB) could be pipetted into separated layers without mixing of their internal contents. When these pattered layers were made inside impermeable walls with only one side exposed, the release of the encapsulants by a compartment by compartment destruction would be expected to be determined by the order of the exposed interfaces resulting in sequential release of content over time (**Figure** 5a). For convenience, centrifuge tubes (0.5 mL) were used as holders for the layered LHMC systems due to their impermeable plastic walls which were also not affected by the LHMC, and had an open top for directional exposure. Due to the conical shape of the centrifuge tube, the surface area to volume ratio would not be consistent throughout the tube so agarose (2%) was first added to the bottom conical section of the tube. MB-LHMC (200 µL, MB at 0.25 mg mL^{-1}) was layered on top of the solidified agarose after which AR-LHMC (200 µL, AR at 1 mg mL^{-1}) was layered on top of the MB-LHMC. Finally, the tube was sealed with further agarose (2%) to prevent the LHMC from leaving the tube while providing a porous matrix for dye and surfactants to pass through. The striped MB-LHMC/AR-LHMC was added to a solution of Tween 20 (30 mM). The result was a sequential release of encapsulants, with AR-LHMC at the closest point to the external environment, AR was released first. Visually the degradation of the LHMC's structure could be observed over time as the layers got gradually smaller over 8 days (Figure 5b). The Single entry point resulted in far slower release of the encapsulants due to the significantly reduced exposed surface area to volume ratio. After the first 2 days, the AR-LHMC layer had almost completely gone but the MB-LHMC layer remained unchanged (Figure 5b, day 2), though the MB-LHMC layer started gradually rescuing after this time until its complete destruction and release on day 8. Quantitively, the external solution was

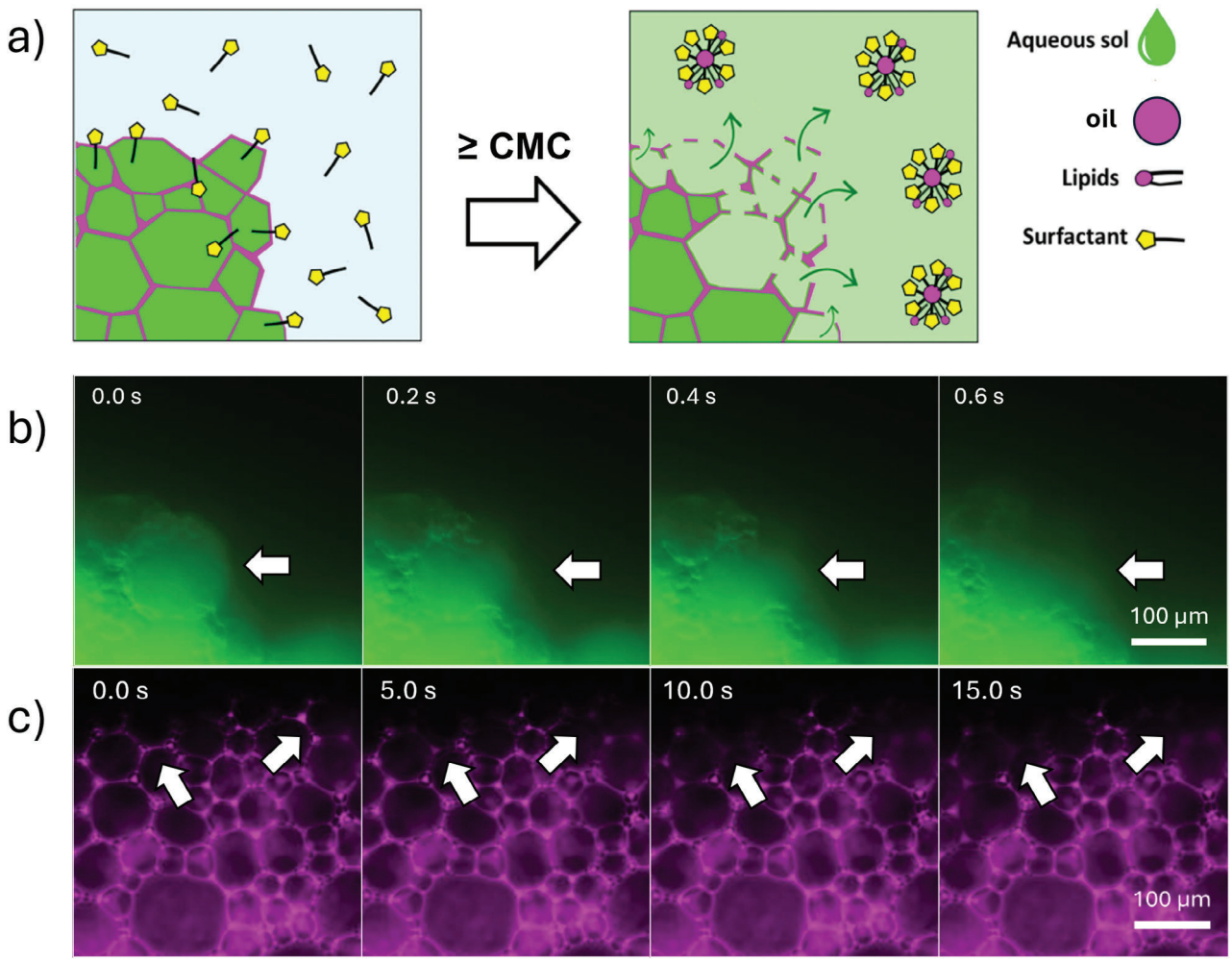

Figure 4. (a) Schematic for LHMC with encapsulated green dye with surfactant concentrations below the CMC and the membrane intact (left) or above the CMC and the membrane being solubilized and compartment release (right). (b) Fluorescence micrographs of LHMC encapsulated aqueous phase, showing a single compartment breaking over 0.6 s, white arrow highlights specific compartment. (c) Fluorescence micrographs of LHMC hydrophobic membrane breaking down over 15 s, white arrows highlight deteriorating sections.

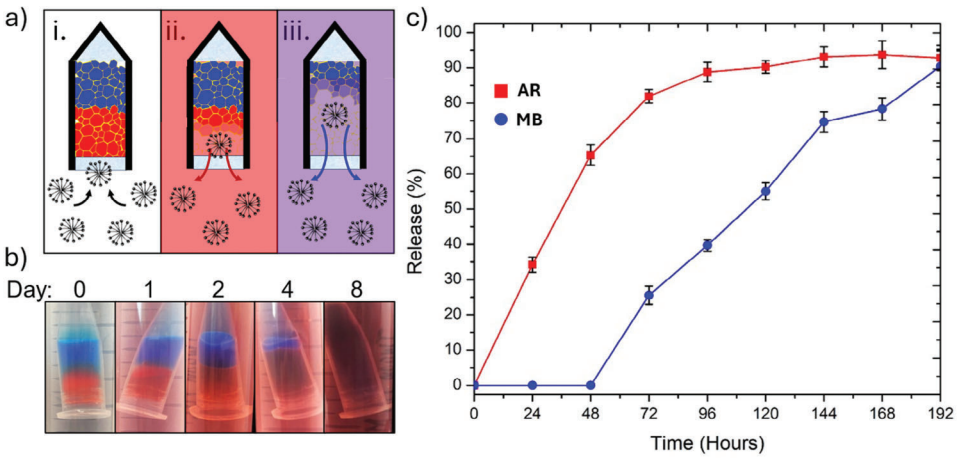

Figure 5. (a) Schematic showing progressive directional membrane solubilization by surfactant micelles leading to pre-determined stages of release, (b) experimental photographs from 0 to 8 days showing progressive release from layered LHMCs, (c) percentage release of AR (red) and MB (blue) from layered LHMCs over 8 days.

measured for release every 12 h for both AR and MB, confirming that as predicted, the initial release was only AR, with MB not being detected in the external solution until after day 2 (Figure 5c). After 48 h, ≈65% of AR had been released but no MB was detected in the external solution. MB would first be detected in the external solution at 72 h by which point the AR had released over 80% of the total amount. Despite the attempt to keep the surface area to volume ratio equal between the two segments, the release rate for AR-LHMC was higher than the release rate for MB-LHMC at 1.15% per hour against 0.75% per hour respectively. We speculate that this may be caused by a slight thickening of the membrane due to molecular rearrangement after compartment breaking, though we could not directly observe this by fluorescence microscopy. We note that while the presence of AR has a concentration-dependent attenuating effect on MB absorption at 668 nm, the MB is only detected when AR has almost fully been released. For this reason, we assume a linear relationship between MB concentration and absorbance (Figure S2, Supporting Information).

3. Conclusion

Here we have demonstrated the use of "lipid-inks" with mechanical agitation for the formation of lipid-hybrid microcompartmentalized (LHMC) systems for efficient encapsulation of aqueous solutions. LHMC systems show high stability in aqueous environments over 6 months of observation and do not release their internal content without external triggers. Release of the encapsulated material can be triggered by membrane solubilization using common commercial surfactants used in food and cosmetic industries, such as sodium dodecyl sulfate (SDS) and Tween 20. Using SDS, an anionic surfactant, the release of the content was also found to be highly dependent on the ionic strength of the solution, due to the change in critical micellization concentration (CMC) point of the SDS. The release of the contents of LHMC-agarose devices in the presence of even high concentrations of surfactant was found to be dramatically slower than unencapsulated dye's simple diffusion through an agarose matrix. This rate of release difference indicates that the membrane destruction is the rate-limiting step in release. Release of the contents from the LHMC material was observed to occur from compartment by compartment bursting, but only when the membrane is directly in contact with solutions containing surfactant near or above the CMC. Due to the microcellular structure, the release of internal content from the LHMC is not continuous but in fact, microliter bursts from a tightly packed array of microcapsules as the membrane breaks in sections. This compartmentalized release and requirement for direct contact with surfactants allow for temporal control of release by spatial patterning and directional exposure with solubilizing solutions. The spatial arrangement of LHMC was shown to result in temporally controlled release by limiting the area exposed to solubilizing solutions, resulting in a sequential release pattern in the order of days. We believe that the environmental ionic strength dependency for release, coupled with the rate limiting and spatial patterning of the LHMC systems may have potential use in applications such as transdermal patches for delivery of polydrugs with pre-programmed release schedules. This could offer several benefits including variable release rates dependent on perspiration, combining drugs co-interacting drugs and patches which need less frequent user replacement for convenience. Future work will aim to develop this material into more practical devices.

4. Experimental Section

Materials: Ethanol (99.5%), chloroform (99%), Alizarin Red, and methylene blue were purchased from FUJIFILM Wako Pure Chemical Corporation, Inc., Japan. Hexadecane (97%), Sodium dodecyl sulfate SDS (98%), Tween20, sodium chloride (99.5%), and Nile Red were purchased from Wako Pure Chemical Industries, Ltd., Japan. 1-palmitoyl-2-oleoyl-sn-glycero-3-phosphocholine (POPC) was purchased from Nippon Oil & Fats Co., Japan. Sorbitan Monooleate (Span80) was purchased from Tokyo Chemical Industry Co., Japan. Calcein fluorescent green dye was purchased from DOJINDO LABORATORIES, Inc., Japan. Phosphate-buffered saline (PBS) was purchased from Thermo Fisher Scientific Inc., the United States. The 3D printing UV-sensitive resin (Basic UV wavelength 405 nm) was purchased from ANYCUBIC, Inc., China. Hexadecyltrimethylammonium bromide (CTAB) and Brij 58 were bought from Sigma-Aldrich, USA. Triton X-100 was bought from MP Biomedicals, USA.

LHMC Formation: LHMCs were formed by applying a "lipid-ink" comprised of lipid Span 80 (2 vol%), POPC (6.5 mM), Nile red (0.16 mM) in hexadecane chloroform and ethanol (75%, 20%, and 5%, respectively). The lipid-inks were pipetted directly onto the desired aqueous solution at 12% to 88% respectively, and vortexed for 10–15 s (**Figure 6a**).

Hydrogel Casing: Agarose casings for the LHMC were formed by use of a custom 3D printed mold to help form a hollow hydrogel structure that could hold LHMC (Figure 6b i,c: left). The 3D mold was assembled to form the inverted shape of the desired final form and hot liquid agarose (2 wt.%) was poured into the mold and allowed to cool at 4 °C for 10 m to solidify (Figure 6b ii). The 3D-printed mold was subsequently disassembled and the agarose casing was gently removed from the mold (Figure 6b iii,c: middle) enabling the desired LHMC volume to be pipetted into the agarose cavity (Figure 6b iv). Finally, the device was sealed by pipetting further hot liquid agarose (2 wt.%) to fill the cavity and again cooling at 4 °C for 10 m to solidify (Figure 6b v,c: right).

Drug Model Release: Agarose-LHMC devices were placed in 15-mL tubes, and submerged in DI water (9 mL), before adding 1 mL of a 10x concentrated PBS solution supplied by Thermo Fisher Scientific Inc, to achieve the desired PBS buffer solution concentration by dilution. Due to the low weight percentage agarose and small volumes of oil, for simplicity, it did not consider displacement of the water due to the devices in the calculations for the concentrations. Solutions were kept at room temperature (24 °C) for the duration of the experiments and not moved or agitated between measurements. For quantification, at set intervals, 1 mL was taken out, the absorbance was measured in a spectrophotometer and then returned to the tube to minimize volume changes and resulting concentration differences. Absorbance measurements were taken at wavelengths of 490 668 nm for Allura Red and methylene blue respectively. Calibration curves showing the relationship between concentration and absorbance are given in the SI (Figure S2, Supporting Information).

Surface Tension Measurement: Surface tension measurements were done with a Krüss K11 (model MK4) Tensiometer using the Du Noüy ring method (Wire diameter 0.37 mm, radius = 9.545 mm) and a Julabo F12 circulation chiller/heater (set to 24 °C). Prior to measurement the Platinum ring was washed with pure deionized water using a wash bottle to wash off any sample residue, subsequently, the ring was briefly flamed off in a blue flame until glowing red with a flame torch to ensure any contamination was burned off. The ring was then left to cool and placed back on the tensiometer microbalance. The samples were poured into a glass dish that had been previously cleaned and measured with pure water to ensure no surfactant contamination was in the dish after testing with water the dish was air dried and the sample was put into the dish total volume ca. 10 mL. The samples were measured until the tensiometer measured at least 10 values with a minimum standard deviation of 0.05 mN m^{-1} (resulting in a ca. 40-minute sample measurement time). The immersion

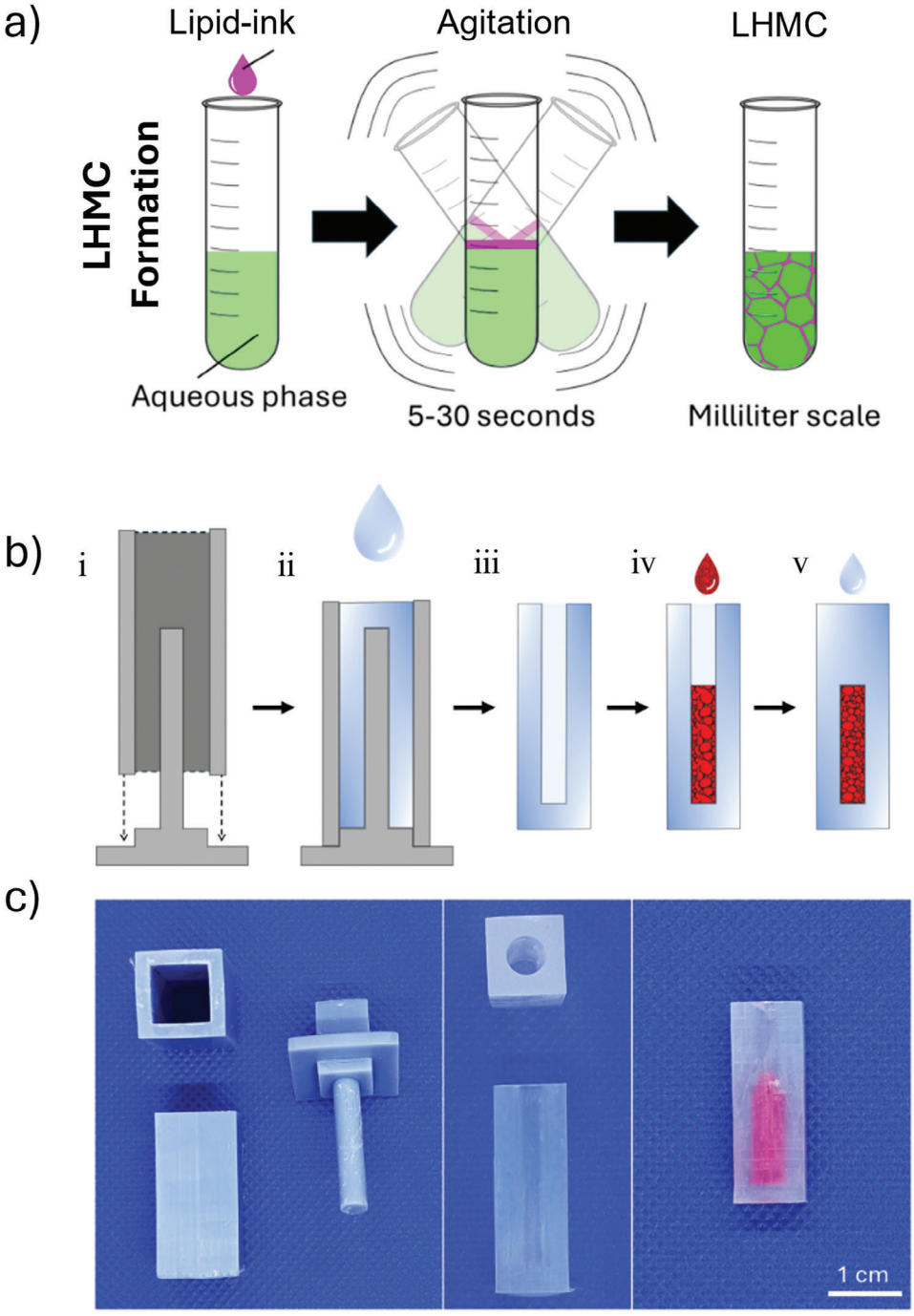

Figure 6. (a) LHMC formation by agitating a lipid-ink (pink) on an aqueous solution (green). Agarose-LHMC device creation procedure. (b) Schematic for creating Agarose-LHMC, i assembling the mold, ii. Adding liquid agarose, iii. Agarose cooling to solidify and removal of plastic mold, iv. Adding LHMC (containing red dye), v. sealing device by further agarose addition (c) left: 2 pieces of the 3D printed mold, left image showing side and top view of the same piece, middle: Resulting agarose device and agarose gel, right: Agarose-LHMC with encapsulated Allura Red dye.

depth of the probe was set to 2 mm with a measurement sensitivity of 0.003 g and the density of the sample was considered to be equal to that of water at 0.998 g cm^{-3}. The platinum ring was submerged in each solution and slowly lifted out (3 mm min^{-1}), measuring the force required to detach it from the liquid surface. All experiments were performed at 24 °C.

Spatial to Temporal Controlled Release: 200 µL of 2% agarose gel was poured into a 1 mL centrifuge tube and kept at 4 °C for 10 m to cure the agarose gel. This process was performed to fill the conical tip of the tube ensuring a constant cross-sectional area of the centrifuge tube. Sequentially, 200 µL of the prepared Methylene Blue LHMC was poured in and

stored at 4 °C for 10 m, then the process was repeated with 200 µL of Allura Red LHMC. Finally, 100 µL of 2% agarose gel was added and cooled at 4 °C for 10 m to seal the device. The prepared samples were submerged into 10 mL of the desired solution and analysis on the external solution was performed by UV-vis spectroscopy to measure release of encapsulated dyes over time.

Instruments: Confocal microscopy was performed using a Zeiss LSM980. Vortexing was performed using a Vortex Genie 2. 3D printing was conducted using the Whale3 Ultra from NOVA3D. Photographs were taken using a Pixel 4 phone camera. Time-lapse images were taken by ELP Megapixel USB camera. Absorbance measurement was performed using a V-630 BIO spectrophotometer.

Supporting Information

Supporting Information is available from the Wiley Online Library or from the author.

Acknowledgements

This work was supported by JSPS KAKENHI Grant Numbers 20H05701, 24H00070, 20H05970, 23K17485 (SMN).

Conflict of Interest

The authors declare no conflict of interest.

Data Availability Statement

The data that support the findings of this study are available from the corresponding author upon reasonable request.

Keywords

controlled release, encapsulation, lipids, membrane, multicompartment

Received: November 29, 2024
Revised: February 4, 2025
Published online:

[1] Q. Zhang, S. Li, Y. Yang, Y. Shan, H. Wang, *Biophys. Rep.* **2021**, *7*, 384.
[2] J. C. Bozelli, R. M. Epand, *J. Mol. Biol.* **2020**, *432*, 5124.
[3] J. R. Winnikoff, D. Milshteyn, S. J. Vargas-Urbano, M. A. Pedraza-Joya, A. M. Armando, O. Quehenberger, A. Sodt, R. E. Gillilan, E. A. Dennis, E. Lyman, S. H. D. Haddock, I. Budin, *Science* **2024**, *384*, 1482.
[4] C. Dias, J. Nylandsted, *Cell Discov.* **2021**, *7*, 4.
[5] D. A. Los, N. Murata, *Biochim. Biophys. Acta (BBA), Biomembr.* **2004**, *1666*, 142.
[6] D. Marsh, *Chem. Phys. Lipids* **2006**, *144*, 146.
[7] K. Kamiya, S. Takeuchi, *J. Mater. Chem. B* **2017**, *5*, 5911.
[8] T. Trantidou, M. S. Friddin, A. Salehi-Reyhani, O. Ces, Y. Elani, *Lab Chip* **2018**, *18*, 2488.
[9] T. Trantidou, M. Friddin, Y. Elani, N. J. Brooks, R. V. Law, J. M. Seddon, O. Ces, *ACS Nano* **2017**, *11*, 6549.
[10] Y. Sato, Y. Hiratsuka, I. Kawamata, S. Murata, S. M. Nomura, *Sci. Robot.* **2017**, *2*, eaal3735.
[11] T. Kojima, K. Terasaka, K. Asakura, T. Banno, *Colloids Surf. Physicochem. Eng. Asp.* **2023**, *669*, 131512.
[12] L. Sercombe, T. Veerati, F. Moheimani, S. Y. Wu, A. K. Sood, S. Hua, *Front. Pharmacol.* **2015**, *6*, 286.
[13] P. Machy, L. D. Leserman, *Biochim. Biophys. Acta (BBA) Biomembr.* **1983**, *730*, 313.
[14] T. B. Gandek, L. van der Koog, A. Nagelkerke, *Adv. Healthcare Mater.* **2023**, *12*, 2300319.
[15] C. Furusawa, K. Kaneko, *Phys. Rev. Lett.* **2000**, *84*, 6130.
[16] D. Kaiser, *Annu. Rev. Genet.* **2001**, *35*, 103.
[17] A. F. Mason, N. A. Yewdall, P. L. W. Welzen, J. Shao, M. van Stevendaal, J. C. M. van Hest, D. S. Williams, L. K. E. A. Abdelmohsen, *ACS Cent. Sci.* **2019**, *5*, 1360.
[18] A. Verma, S. G. Jena, D. R. Isakov, K. Aoki, J. E. Toettcher, B. E. Engelhardt, *Proc. Natl. Acad. Sci.* **2021**, *118*, 2026123118.
[19] R. J. Archer, S. Hamada, R. Shimizu, S.-I. M. Nomura, *Langmuir* **2023**, *39*, 4863.
[20] N.-N. Deng, M. Yelleswarapu, W. T. S. Huck, *J. Am. Chem. Soc.* **2016**, *138*, 7584.
[21] M. S. Friddin, G. Bolognesi, Y. Elani, N. J. Brooks, R. V. Law, J. M. Seddon, M. A. A. Neil, O. Ces, *Soft Matter* **2016**, *12*, 7731.
[22] Y. Elani, R. V. Law, O. Ces, *Phys. Chem. Chem. Phys.* **2015**, *17*, 15534.
[23] Y. Elani, R. V. Law, O. Ces, *Nat. Commun.* **2014**, *5*, 5305.
[24] C. Yang, Y. Yu, X. Wang, Q. Wang, L. Shang, *Eng. Regen* **2021**, *2*, 171.
[25] B. J. Anaya, J. R. Cerda, R. M. D'Atri, I. Yuste, F. C. Luciano, A. Kara, H. K. Ruiz, M. P. Ballesteros, D. R. Serrano, *Int. J. Pharm.* **2023**, *642*, 123194.
[26] A. P. Haring, Y. Tong, J. Halper, B. N. Johnson, *Adv. Healthcare Mater.* **2018**, *7*, 1800213.
[27] C. Karavasili, S. Babaee, S. Kutty, J. N. Chu, S. Min, N. Fitzgerald, J. Morimoto, N. Inverardi, G. Traverso, *Adv. Healthcare Mater.* **2023**, *12*, 2301101.
[28] T. McDonagh, P. Belton, S. Qi, *Int. J. Pharm.* **2023**, *637*, 122895.
[29] A. Patel, D. Ojji, H. A. de Silva, S. MacMahon, A. Rodgers, *Nat. Med.* **2022**, *28*, 226.
[30] Z. Luo, J. Che, L. Sun, L. Yang, Y. Zu, H. Wang, Y. Zhao, *Eng. Regen.* **2021**, *2*, 257.
[31] D. Cao, X. Chen, F. Cao, W. Guo, J. Tang, C. Cai, S. Cui, X. Yang, L. Yu, Y. Su, J. Ding, *Adv. Funct. Mater.* **2021**, *31*, 2100349.
[32] G. Xu, Y. Lu, C. Cheng, X. Li, J. Xu, Z. Liu, J. Liu, G. Liu, Z. Shi, Z. Chen, F. Zhang, Y. Jia, D. Xu, W. Yuan, Z. Cui, S. S. Low, Q. Liu, *Adv. Funct. Mater.* **2021**, *31*, 2100852.
[33] Y. Yang, L. Xu, D. Jiang, B. Z. Chen, R. Luo, Z. Liu, X. Qu, C. Wang, Y. Shan, Y. Cui, H. Zheng, Z. Wang, Z. L. Wang, X. D. Guo, Z. Li, *Adv. Funct. Mater.* **2021**, *31*, 2104092.
[34] S. M. Nomura, R. Shimizu, R. J. Archer, G. Hayase, T. Toyota, R. Mayne, A. Adamatzky, *ChemSystemsChem* **2022**, *4*, 202200006.
[35] J. Juan-Colás, L. Dresser, K. Morris, H. Lagadou, R. H. Ward, A. Burns, S. Tear, S. Johnson, M. C. Leake, S. D. Quinn, *Langmuir* **2020**, *36*, 11499.
[36] S. A. Morton III, D. J. Keffer, A. N. Davis, R. M. Counce, *Sep. Sci. Technol.* **2008**, *43*, 310.
[37] P. Gaddam, W. Ducker, *Langmuir* **2019**, *35*, 5719.
[38] M. J. Qazi, S. J. Schlegel, E. H. G. Backus, M. Bonn, D. Bonn, N. Shahidzadeh, *Langmuir* **2020**, *36*, 7956.
[39] K. D. Danov, P. A. Kralchevsky, K. P. Ananthapadmanabhan, *Adv. Colloid Interface Sci.* **2014**, *206*, 17.